MOLECULAR AND CELLULAR BIOLOGY, Aug. 2011, p. 3094–3104 Vol. 31, No. 15
0270-7306/11/$12.00 doi:10.1128/MCB.01449-10

Nonallelic Transcriptional Roles of CTCF and Cohesins at Imprinted Loci[▽]

Shu Lin,[1] Anne C. Ferguson-Smith,[2] Richard M. Schultz,[3] and Marisa S. Bartolomei[1]*

Department of Cell and Developmental Biology, University of Pennsylvania School of Medicine, Philadelphia, Pennsylvania 19104[1]; Department of Physiology, Development and Neuroscience, University of Cambridge, Cambridge CB2 3EG, United Kingdom[2]; and Department of Biology, University of Pennsylvania, Philadelphia, Pennsylvania 19104[3]

Received 20 December 2010/Returned for modification 29 January 2011/Accepted 17 May 2011

The cohesin complex holds sister chromatids together and is essential for chromosome segregation. Recently, cohesins have been implicated in transcriptional regulation and insulation through genome-wide colocalization with the insulator protein CTCF, including involvement at the imprinted *H19*/*Igf2* locus. CTCF binds to multiple imprinted loci and is required for proper imprinted expression at the *H19*/*Igf2* locus. Here we report that cohesins colocalize with CTCF at two additional imprinted loci, the *Dlk1-Dio3* and the *Kcnq1*/*Kcnq1ot1* loci. Similar to the *H19*/*Igf2* locus, CTCF and cohesins preferentially bind to the *Gtl2* differentially methylated region (DMR) on the unmethylated maternal allele. To determine the functional importance of the binding of CTCF and cohesins at the three imprinted loci, CTCF and cohesins were depleted in mouse embryonic fibroblast cells. The monoallelic expression of imprinted genes at these three loci was maintained. However, mRNA levels for these genes were typically increased; for *H19* and *Igf2* the increased level of expression was independent of the CTCF-binding sites in the imprinting control region. Results of these experiments demonstrate an unappreciated role for CTCF and cohesins in the repression of imprinted genes in somatic cells.

A number of mammalian genes termed imprinted genes are expressed exclusively from one parental allele, and many of these genes are important for embryonic development. The aberrant expression of these genes is associated with human cancers and genetic diseases, such as Beckwith-Wiedemann syndrome (BWS), Silver-Russell syndrome, Prader-Willi syndrome, and Angelman syndrome (4). Imprinted gene expression requires the establishment of imprinting marks in the germ line and early embryo and, subsequently, the maintenance of these marks during cell division in somatic tissues. To date, approximately 100 imprinted genes have been identified, and many are located in 1-Mb clusters that harbor differentially methylated regions (DMRs) (for a review, see reference 2). Within a cluster, imprinted gene expression is coregulated by a *cis*-acting regulatory element, termed an imprinting control region (ICR), that is also a DMR. There are two major mechanisms that regulate imprinted gene clusters. One mechanism requires the transcription of a long noncoding RNA (ncRNA), which silences genes in *cis*, allowing the alternate allele to be expressed. This study focuses on the second mechanism, which employs allele-specific insulation mediated by the insulator protein CTCF.

CTCF is a highly conserved 11-zinc-finger protein, which was initially identified as a CCCTC binding factor in the chicken c-*myc* locus (36). CTCF is implicated in transcriptional activation, repression, and insulation (for a review, see reference 15). In addition, CTCF facilitates inter- and intrachromosomal interactions (68). CTCF binds to the *H19*/*Igf2* ICR in a DNA methylation-sensitive manner (3, 21, 27, 55). In this case, CTCF mediates the insulator activity of the unmethylated maternal ICR by blocking the *Igf2* promoter from engaging enhancers downstream of *H19* that are shared by *H19* and *Igf2*. The deletion or mutation of the four CTCF-binding sites within the ICR causes a paternalization of the maternal allele, *Igf2* biallelic expression, and *H19* repression (12). In addition to the *H19*/*Igf2* locus, CTCF binds to DMRs at a number of imprinted loci, including *Gtl2*, *Kcnq1*/*Kcnq1ot1*, *Grb10*, and *Rasgrf1* (16, 22, 29, 70). CTCF binding appears to be methylation sensitive at the KvDMR1 region in the *Kcnq1*/*Kcnq1ot1* locus as well as the *Grb10* and *Rasgrf1* loci (16, 22, 70). Interestingly, the *Kcnq1*/*Kcnq1ot1* locus and, possibly, the *Gtl2* locus use the ncRNA mechanism to regulate imprinted expression (see below), whereas imprinting regulation at the *Grb10* and *Rasgrf1* loci remains unclear. Furthermore, the depletion of CTCF in mouse oocytes led to a reduction in *Gtl2* and *Grb10* RNA levels (65). It is intriguing that CTCF is present and may possibly function at imprinted loci that are regulated by different imprinting control mechanisms (insulator versus ncRNA). Nevertheless, it is still incompletely understood how CTCF manifests its insulator function at the *H19*/*Igf2* locus and whether it has a similar function at other imprinted loci.

Recently, we and others reported the genome-wide colocalization of CTCF and cohesin complex subunits, including that at the *H19* ICR (43, 48, 54, 67). Those studies suggested that cohesins bind to the DNA through a consensus sequence similar to that of CTCF. Cohesins are required for sister chromatid cohesion during cell division. The mitotic cohesin complex consists of four subunits, SMC1/SMC1A, SMC3, RAD21/SCC1, and SCC3 (SA1/SA2), which were previously proposed to form a ringlike structure and encircle the sister chromatids during mitosis (19). Recent studies of *Saccharomyces cerevisiae* and higher organisms suggested that cohesins are also involved in transcriptional regulation, chromatin structure, and devel-

* Corresponding author. Mailing address: Department of Cell and Developmental Biology, University of Pennsylvania School of Medicine, CRB 363, Philadelphia, PA 19104. Phone: (215) 898-9063. Fax: (215) 573-6434. E-mail: bartolom@mail.med.upenn.edu.

▽ Published ahead of print on 31 May 2011.

TABLE 1. Primers and enzymes used for allele-specific analysis by PCRs[a]

Region or gene	Primer or probe (sequence)	Temp (°C)	SNP B/C	Enzyme	Product size(s) (bp)
IG-DMR	IG-DMR207 (TACGGAGATGTGCTGTGGAC) IG-DMR442 (CTCGCTAGTTCACGGAGGTC)	62	A/G	NcoI	B, 104, 95, 37 C, 199, 37
Gtl2 DMR	Gtl2 1915F (TGAAACCTGTTGGGCG) Gtl2 2158R (CAATGGGAGGGGTACAGATG)	61	T/C	HaeII	B, 109, 70, 48, 17 C, 97, 70, 48, 17, 12
KvDMR CTCF BS1	KvDMR 2701F (CCCACCGAAGTAATCCAAAA) KvDMR 3098R (TCAGCTAGGAAGGGATGAGG)	62	C/T	Hpy188I	B, uncut, 398 C, 292, 106
KvDMR CTCF BS2	KvDMR 2258F (CTGAGAAGCCAAGTGGATCG) KvDMR 2553R (CCACCAGCCTCAGCATATTT)	62	A/G	MfeI/Tsp509I	B, 214, 82 C, uncut, 296
H19	HI3 (CCTCAAGATGAAAGAAATGGT) HE5 (AACACTTTATGATGGAACTGC) Probe Mut (CCACCTGTCGTCCATCTCC-FL) Probe Anc (RED640-TCTGAGGGCAACTGGGTGTGG-P)	55	G/A	NA, real-time PCR	NA, real-time PCR
	HE2 (TGATGGAGAGGACAGAAGGG) HE4 (TTGATTCAGAACGAGACGGAC)	55	G/A	Cac8I	B, 173, 62 C, uncut, 235
Igf2	Igf18 (ATCTGTGACCTCTTGAGCAGG) Igf20 (GGGTTGTTTAGAGCCAATCAA)	58		Tsp509I	B, 180, 20 C, 165, 20, 15
Gtl2	Gtl3 (CCAAAGCCATCATCTGGAATC) Gtl4 (CAGCCCTGTGAGGTAGGAAC)	55	T/?	SfcI	B, 250, 87 C, uncut, 337
Dlk1	Dlk2up (CTGGCTTTCTTCCCGCTGGAC) Dlk317dn (GACACAGCCAGGGGCAGTTA)	54	T/C	DraIII	B, 212, 104 C, uncut, 316

[a] SNP, single-nucleotide polymorphism; B, B6 maternal allele; C, paternal allele; NA, not applicable.

opment (for a review, see reference 9), likely through their ability to interact with chromosomes. *Drosophila melanogaster* SMC1, RAD21, and SCC3 were suggested previously to prevent enhancer-promoter interactions at the *cut* locus (10, 47), indicating that cohesins function as insulator proteins. Taken together, the genome-wide colocalization of CTCF and cohesins as well as the noncanonical roles of cohesins in transcription regulation provide a clue for the possible mechanism underlying the function of CTCF in chromosome biology.

We demonstrated that the binding of cohesin complex subunits to the *H19* ICR requires the CTCF-binding sites (54), suggesting that CTCF and cohesins may function in concert to regulate the imprinted expression of *H19* and *Igf2*. Additionally, RNA interference (RNAi) experiments with HeLa cells and a human breast epithelial cell line (HB2 cells) revealed similar expression changes of the *H19*/*Igf2* locus genes when CTCF knockdown (KD) and cohesin KD cells were compared (42, 67). Those studies suggested that cohesins are involved in the imprinted regulation of the *H19*/*Igf2* locus. However, HeLa cells and HB2 cells express low levels of *H19* and *Igf2*; thus, the maintenance of imprinted expression may not be tightly regulated. Moreover, the changes observed by these studies could be due to indirect effects rather than a perturbed function of cohesins in imprinting.

To investigate further the role of CTCF and cohesins in genomic imprinting and insulator function, we used a primary embryonic cell type, mouse embryonic fibroblasts (MEFs), and expanded our studies to two DMRs at additional CTCF-bound imprinted loci, the *Gtl2* DMR and KvDMR1. We show that cohesin complex subunits also bind these DMRs in MEFs, and similar to the *H19*/*Igf2* locus, CTCF and cohesins preferentially bind to the unmethylated allele of the *Gtl2* DMR. However, CTCF and cohesins bind biallelically to KvDMR1. To investigate the roles of CTCF and cohesins in these imprinted loci, we performed RNAi experiments targeting CTCF and two cohesin complex subunits in MEFs and found that the *Igf2* expression level is elevated but remains imprinted, suggesting an indirect effect of cohesin depletion at the *H19*/*Igf2* locus. We propose that cohesins are involved in the regulation of proper expression levels of imprinted genes rather than having a direct role in imprinting.

MATERIALS AND METHODS

Isolation and culture of F1 hybrid MEFs. MEFs were isolated from individual mouse 14.5-day-postcoitus (dpc) embryos generated from crosses between C57BL/6 (B6) (for both the wild-type and the $H19^{\Delta R/+}$ mutant) females and males with *Mus musculus castaneus* (C) chromosome (Chr) 7, distal 12 and X, in a B6 background [B6(CAST7P12X)], as previously described (64). The $H19^{+/\Delta R}$ MEFs were generated from crosses between female with *Mus musculus castaneus* (C) chromosome 7 in a B6 background [B6(CAST7)] and B6 males as previously described (40).

Chromatin immunoprecipitation. Chromatin immunoprecipitation (ChIP) assays were carried out by using a chromatin immunoprecipitation assay kit (catalog numbers 17-295 and 17-610; Upstate) according to the manufacturer's instructions and as previously described (64). Approximately 1×10^6 MEFs were used in each immunoprecipitation, which resulted in 40 to 100 μg of chromatin-immunoprecipitated (ChIPed) DNA. All PCR primers and conditions are listed in Tables 1 and 2.

siRNA treatments. MEFs were cultured in 24-well plates and treated every 48 h with two to three sequential small interfering RNA (siRNA) treatments. Cells were trypsinized and plated at 30 to 40% confluence. A total of 40 to 80 pM siRNAs was mixed with 1 μl Lipofectamine 2000 (Invitrogen) and 100 μl Opti low-serum medium (Invitrogen) and added to the medium (high-glucose Dulbecco's modified Eagle's medium [DMEM] plus 10% fetal bovine serum [FBS]) upon cell plating. The following siRNAs were used: control siRNA (catalog

TABLE 2. Primers and PCR conditions used for real-time PCRs

Region or gene	Primer	Temp (°C)	Primer concn (μM)	$MgCl_2$ concn (mM)
IG-DMR	IG-DMR207 (TACGGAGATGTGCTGTGGAC) IG-DMR442 (CTCGCTAGTTCACGGAGGTC)	62	0.3	1.25
Gtl2 DMR	Gtl2 1998F (TGGTTGGGCTATTGGAGTCT) Gtl2 2158R (CAATGGGAGGGGTACAGATG)	61	0.5	3
KvDMR Ctrl-1	KvDMR 3025F (TACAGGATTGTACGACCTAG) KvDMR 3220R (AGAGCCAGGGGCATACTCAT)	63	0.3	3.5
KvDMR CTCF BS-1	KvDMR 2644F (ACCATGCAGAGAAAAGCACA) KvDMR 2844R (CTAGCCGTTGTCGCTAGGAG)	56	0.4	5
KvDMR CTCF BS-2	KvDMR 2258F (CTGAGAAGCCAAGTGGATCG) KvDMR 2553R (CCACCAGCCTCAGCATATTT)	62	0.2	3
KvDMR Ctrl-2	KvDMR 1762F (CACTCACCTTGGGACTCGAC) KvDMR 2007R (AGAAGCAGAGGTGATTCGTG)	58	0.6	4
Ctcf	CTCF5F1 (GCCAGCAGGGACACATACAAG) CTCF5R1 (GCTTTCGCAAGTGGACACC)	56	0.5	3.5
Smc1	Smc1 3767 (CAAGTACCCAGATGCCAACC) Smc1 3983 (CGATCCATGATAGGGGGTAA)	55	0.4	2
Rad21	Rad21 2815 (CAAGGCTGCACACTCCTGTA) Rad21 3045 (CCCCATAAAAGTGCCAACAC)	55	0.3	2.5
H19	HE2 (TGATGGAGAGGACAGAAGGG) HE4 (TTGATTCAGAACGAGACGGAC)	55	0.4	4.5
Igf2	Igf2f (CGCTTCAGTTTGTCTGTTCG) Igf2r (GCAGCACTCTTCCACGATG)	58	0.25	2.4
Gtl2/Meg3	Meg3f (TTGCTGTTGTGCTCAGGTTC) Meg3r (ATCCTGGGGTCCTCAGTCTT)	60	0.4	2
Dlk1	Dlk1f (CGGGAAATTCTGCGAAATAG) Dlk1r (TGTGCAGGAGCATTCGTACT)	60	0.4	1.25
Arpp0	Arpp0#72L (TCCCACTTACTGAAAAGGTCAAG) Arpp0#72R (TCCGACTCTTCCTTTGCTTC)	55	0.4	4.5

number 12935-300; Invitrogen), CTCF siRNA (Stealth Ctcf-MSS203343; Invitrogen), Smc1 siRNA (Smc1a-MSS216158; Invitrogen), and Rad21 (RAD21 On-Target Plus siRNA J-058531-12; Dharmacon). For each experiment, at least three biological replicates were generated and analyzed.

Western blots. Cells were lysed with TNE buffer (100 mM Tris [pH 7.4], 1% NP-40, 10 mM EDTA) with a 1:100 dilution of proteinase inhibitor cocktail (Sigma) and 1 mM dithiothreitol (DTT). Lysates were mixed with 5× loading buffer, denatured by heating at 95°C for 10 min, and fractionated on an 8% SDS-PAGE gel. The protein was transferred onto a nitrocellulose membrane (Bio-Rad), blocked in 3% nonfat milk (Bio-Rad) in Tris-buffered saline (TBS)–Tween (TBST) (0.05% Tween 20 in 1× TBS), and probed with primary and secondary antibodies (horseradish peroxidase [HRP]-conjugated anti-mouse and anti-rabbit antibody; GE). The blot was visualized by using chemiluminescence (ECL Plus; GE). Quantification was performed by using ImageJ software (NIH).

RNA extraction and reverse transcription. Total RNA from MEFs was extracted by using an RNeasy Microkit (Qiagen) according to the manufacturer's instructions. The reverse transcription (RT) reaction, primed with random primers, was performed by using Superscript II or III reverse transcriptase (Invitrogen) according to the manufacturer's instructions. For each sample, the minus-RT control was done without Superscript II or III and confirmed to be negative by PCR of the glyceraldehyde-3-phosphate dehydrogenase (GAPDH) gene.

Real-time PCRs and statistical analysis. Real-time PCR analysis was carried out with the LightCycler real-time PCR system (Roche), as previously described (64), with a few modifications. Reaction mixtures were set up in duplicates or triplicates by using Ready-To-Go PCR beads (Amersham) with a 5-min initial incubation with TaqStart antibody (Clontech), followed by the addition of 0.2 to 0.6 μM primers (Table 2), 1× EvaGreen (Biotium), and 1.25 to 5 mM $MgCl_2$. Data analysis was performed by using Light Cycler 4.0 software using the Relative Quantification program (Monocolor) to determine the ratio of each ChIP sample relative to input or cDNA levels relative to the acidic ribosomal phosphoprotein P0 (*Arpp0*), β-actin, or GAPDH gene (64, 66). For statistical analysis, the two-tail paired Student *t* test was used, and differences with a P value of <0.05 were considered significant.

Allele-specific analysis of ChIPed DNA by PCRs and restriction enzyme digestions. All PCRs were carried out with Ready-To-Go PCR beads (Amersham) using 0.3 μM each primer (Table 1) and 0.1 μCi of [^{32}P]dCTP. Products were digested (Table 1) and resolved on 7% or 12% polyacrylamide gels. Gels were exposed to phosphorscreens and scanned on a Typhoon Trio Phosphorimager (GE). The relative band intensities were quantified by using ImageJ software (NIH).

Allele-specific RNA analysis. *H19* RNA assays were conducted on cDNA using the LightCycler real-time PCR system (Roche Molecular Biochemicals) as described previously (46). *Igf2* and *Gtl2* RNA assays were conducted on cDNA by allele-specific restriction digests as previously described (66). *Dlk1* RNA assays were conducted, with some modifications, as previously described (20). The digested PCR products were resolved by 7% or 12% polyacrylamide gel electrophoresis. The gels were stained with ethidium bromide. The contribution of each parental allele to the total RNA was determined by using Quantity One software (Bio-Rad). All primers used are listed in Table 1.

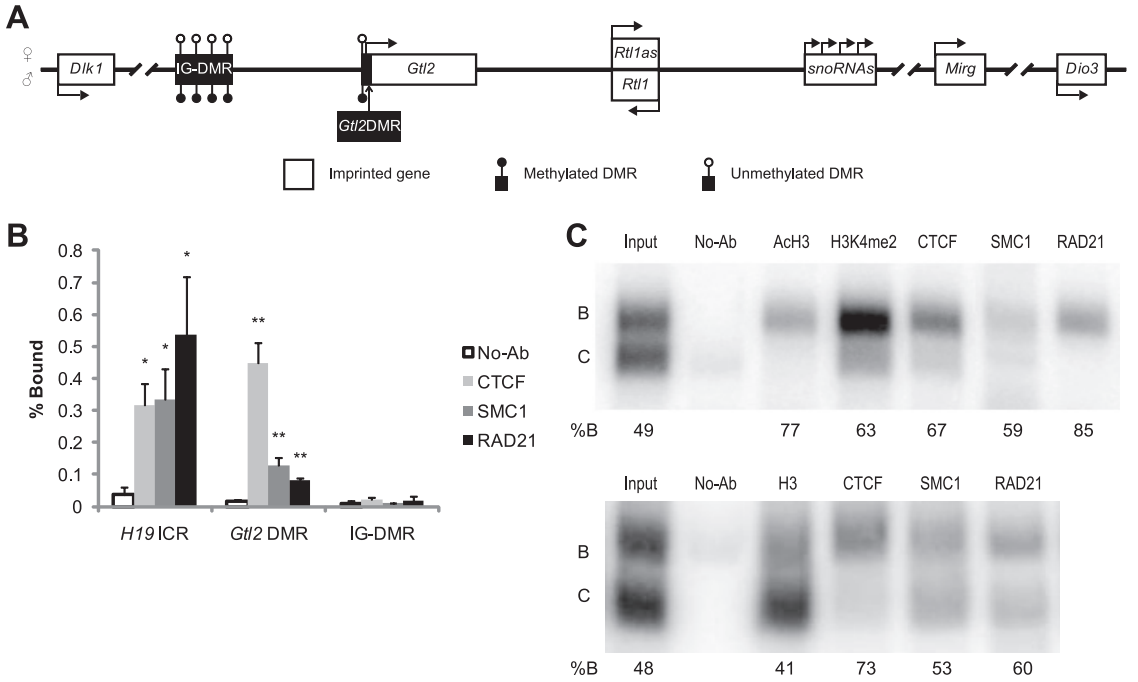

FIG. 1. CTCF and cohesins colocalize at the *Gtl2* DMR in MEFs. (A) Schematic showing the *Dlk1-Dio3* imprinted locus (not to scale). The transcriptional and methylation statuses of the maternal and paternal chromosomes are represented at the top and bottom of the DNA strand, respectively. (B) CTCF and cohesins colocalize at the *Gtl2* DMR but not the IG-DMR. The *H19* ICR is included for comparison. Shown are real-time PCR results from at least three independent ChIP experiments. *, $P < 0.05$; **, $P < 0.01$. *P* values show differences between no-antibody (No-Ab) controls and antibodies against CTCF, SMC1, or RAD21. Error bars indicate standard errors of data from at least three biological replicates. (C) Allele-specific analysis of ChIPed DNA by PCR showing preferential binding of CTCF and cohesins on the maternal *Gtl2* DMR. Two independent experiments are shown. Histone H3, AcH3, and H3K4me2 are included as positive controls. B, maternal allele; C, paternal allele. The percentage of protein binding on the B allele over total binding (B plus C) is indicated at the bottom. At least three experiments were performed, and similar results were obtained.

Antibodies. The following antibodies were used in ChIP and Western blotting (WB): anti-histone H3 (ab1791 [ChIP, 5 μg]; Abcam), anti-acetylated histone H3 (AcH3) (catalog number 06-599 [ChIP, 5 μg]; Millipore), anti-dimethyl-histone H3 lysine 4 (H3K4me2) (catalog number 07-030 [ChIP, 5 μl]; Millipore), anti-CTCF (catalog number 07-729 [ChIP, 5 μl; WB, 1:1,000]; Millipore), anti-SMC1 (catalog number A300-055A [ChIP, 5 μl; WB, 1:1,000]; Bethyl), anti-RAD21 (catalog number A300-080A [ChIP, 5 μl; WB, 1:500]; Bethyl), and anti-α-tubulin (catalog number T6199 [WB, 1:2,000]; Sigma).

RESULTS

Colocalization of CTCF and cohesins at the *Gtl2* DMR and the KvDMR1 region. To determine whether CTCF and cohesins interact and function similarly at multiple imprinted loci, we investigated binding at two independent imprinted loci. *Gtl2* encodes a long ncRNA with multiple spliced forms of unknown function (45, 51). *Gtl2* resides in the *Dlk1-Dio3* imprinting cluster, which was initially identified in a uniparental disomy (UPD) of distal mouse chromosome (Chr) 12 deficiencies (56) and UPDs of the orthologous human Chr 14q32 (23). The locus contains three paternally expressed protein-coding genes (*Dlk1*, *Rtl1*, and *Dio3*) and a number of maternally expressed ncRNAs (Fig. 1A). It was proposed that these ncRNAs can make up a large polycistronic transcription unit that represses the protein-coding genes on the maternal chromosome. In human and mouse, the intergenic DMR (IG-DMR), which is methylated in the male germ line, functions as the ICR of the cluster (25, 34, 35). There is a second postfertilization-derived paternally methylated *Gtl2* DMR, spanning the promoter, exon 1, and part of intron 1 of *Gtl2* (56). The maternal deletion of the *Gtl2* DMR in human results in the regional silencing of imprinted genes (24). The *Gtl2* DMR contains a CTCF-binding site (29, 45), raising the possibility that cohesins bind to the region.

To investigate the binding of CTCF and cohesins at the *Gtl2* DMR, we used quantitative real-time PCR following chromatin immunoprecipitation (ChIP) in F1 hybrid MEFs (see Materials and Methods). At the *Gtl2* DMR, antibodies against CTCF, SMC1, and RAD21 precipitated significantly more chromatin ($P < 0.01$) than the no-antibody negative control. However, no enrichment of CTCF and cohesins was seen at the IG-DMR (Fig. 1B), consistent with the absence of CTCF-binding sites (45). CTCF bound to the *Gtl2* DMR at a level similar to that of the *H19* ICR, whereas not as much SMC1 and RAD21 bound to the *Gtl2* DMR as what bound to the *H19* ICR (Fig. 1B), indicating that the affinities of cohesins differ between the *Gtl2* DMR and the *H19* ICR. Therefore, cohesins may interact with CTCF differently and exhibit disparate functions at these two loci.

To determine if the binding of CTCF and cohesins is exclusive to one parental allele, we performed allele-specific PCR analysis of DNA isolated from ChIP. Because the CTCF-binding site resides near the *Gtl2* promoter, and active histone modifications were reported previously to be associated with

the maternal allele at this region (5), we included two antibodies against acetylated histone H3 (AcH3) and dimethyl-histone H3 lysine 4 (H3K4me2) as controls. AcH3 and H3K4me2 preferentially bind the transcribed, maternal allele (Fig. 1C, top), as do CTCF and the two cohesin complex subunits (Fig. 1C). An antibody against histone H3 was also included; H3 was present at approximately equal levels on the parental alleles (Fig. 1C, bottom). The binding of CTCF on the unmethylated maternal allele is consistent with results of experiments showing a methylation-sensitive binding pattern (15). In conclusion, CTCF and cohesins colocalize in an allele-specific manner at the *Gtl2* DMR, similar to the *H19* ICR.

The *Kcnq1*/*Kcnq1ot1* imprinted locus contains maternally expressed genes and one paternally expressed long ncRNA, *Kcnq1ot1*, which is an antisense transcript of *Kcnq1* (Fig. 2A). The loss of imprinted expression at this locus is the most frequent alteration in individuals with BWS (reviewed in reference 44). This locus uses primarily the ncRNA mechanism to regulate imprinted expression. The maternally methylated KvDMR1 is the ICR of the locus and includes the *Kcnq1ot1* promoter (53). On the paternal allele, where KvDMR1 is unmethylated, *Kcnq1ot1* is expressed, which results in the silencing of the adjacent genes. The paternal deletion of KvDMR1 causes a loss of expression of *Kcnq1ot1* and results in the activation of genes in *cis* in embryonic and extraembryonic tissues (17, 32). The transcription of the intact *Kcnq1ot1* mRNA is required for the imprinted expression of the entire locus (39, 52, 58), with one exception: Shin and colleagues showed previously that *Cdkn1c* imprinting was maintained on a *Kcnq1ot1* truncation allele in several fetal and neonatal tissues (52). Fitzpatrick et al. additionally identified two CTCF-binding sites in KvDMR1 (16). These data, together with evidence that KvDMR1 has insulator and silencer activities *in vitro* (16, 38, 57), indicate that CTCF may form an insulator at KvDMR1 as a secondary mechanism in the *Kcnq1*/*Kcnq1ot1* imprinted locus.

We examined CTCF and cohesin occupancy at KvDMR1, including the two previously reported CTCF-binding sites (CTCF-binding site 1 [CTCF BS-1] and CTCF BS-2) (16) and two negative controls (control 1 [Ctrl-1] and Ctrl-2). KvDMR1 has two CpG islands, as shown in Fig. 2A. The two CTCF-binding sites reside in the first CpG island; Ctrl-1 is located about 150 bp upstream of the first CpG island, whereas Ctrl-2 is in the second CpG island. Following ChIP, real-time PCR analysis showed that CTCF, SMC1, and RAD21 associated with both CTCF BS-1 and -2 but not Ctrl-2 (Fig. 2B). SMC1 was also detected at Ctrl-1 (Fig. 2B), most likely because Ctrl-1 is only about 200 bp away from CTCF BS-1. Allele-specific analyses revealed that the allelic bias of CTCF binding at KvDMR1 in MEFs was very weak, in contrast to AcH3 and H3K4me2, which were strongly biased toward the paternal allele. Compared to the input DNA, CTCF antibody precipitated 5 to 20% more of the paternal allele than the maternal allele. Similarly, the two cohesin complex subunits showed a small bias (~5%) toward the paternal allele (Fig. 2C and D). Our results are in contrast with those of Fitzpatrick and colleagues, who showed that CTCF binding at KvDMR1 was exclusively on the paternal allele in C57BL/6 × SD7 F1 hybrid MEFs (16). These contrasting results could be reflective of mouse strain differences.

Functional analysis of CTCF and cohesins in MEFs. The results described above demonstrated that CTCF and cohesins colocalize at three imprinted DMRs. To assess the functional significance of the binding of CTCF and cohesins in regulating the expression of imprinted genes, we performed RNAi experiments. F1 hybrid MEFs were treated with siRNAs targeting *Ctcf*, *Smc1*, and *Rad21*. An siRNA that does not target any known transcripts in mouse was included as a control. To achieve a better knockdown (KD) efficiency, we tested sequential siRNA treatments by treating the cells every 48 h. Maximum depletion (~75% to 90%) of targeted proteins occurred by 72 h and was maintained for an additional 72 h, with two to three treatments of siRNAs (data not shown). Accordingly, we conducted most of the experiments with two or three sequential siRNA treatments and harvested cells at 96 h to 144 h. Because no obvious growth or proliferation defects were observed in the siRNA-treated cells, any changes in these cells were likely due to the altered function of CTCF and cohesin complex subunits in transcriptional regulation, rather than cell division.

The RNAi approach using two sequential treatments of one siRNA against each transcript successfully reduced the amount of the protein encoded by the targeted mRNA (Fig. 3A). In general, the siRNAs targeting *Ctcf* and *Rad21* had higher KD efficiencies than did the siRNA targeting *Smc1* (Fig. 3A). Furthermore, because there are thousands of CTCF- and cohesin-binding sites in the genome (43, 48, 67), it was possible that the depletion of CTCF and cohesins would affect housekeeping genes. Therefore, we examined the mRNA levels of three housekeeping genes (the β-actin, acidic ribosomal phosphoprotein P0 [*Arpp0*], and GAPDH genes) in the siRNA-treated cells (Fig. 3B) and found that the target mRNA was reduced to 30 to 40% compared to the control siRNA-treated cells. Because no effect on the relative transcript abundance of housekeeping genes was observed, only the *Arpp0* gene was used as the control in subsequent experiments.

We first characterized the effect of the depletion of CTCF and cohesins at the *H19*/*Igf2* locus. We hypothesized that CTCF and cohesins work in concert at the *H19* ICR as insulator proteins and that the depletion of CTCF and/or cohesin complex subunits would reduce the insulator activity, resulting in increased *Igf2* transcription levels due to expression from the normally repressed maternal allele. The deletion of the *H19* ICR or CTCF-binding sites from the maternal chromosome caused a biallelic expression of *Igf2* and a reduction of *H19* RNA levels, indicating competition between *H19* and *Igf2* for the shared enhancers on the maternal chromosome (12, 59, 61). Therefore, we expected to observe reduced *H19* expression levels in CTCF- and/or cohesin-depleted cells. To test this hypothesis, we treated MEFs with individual siRNAs against CTCF and cohesins as well as with different combinations of siRNAs (Fig. 4A and 5A). As expected, *Ctcf* siRNA-treated cells had elevated *Igf2* expression levels ($P < 0.01$), approximately 3-fold relative to those of control siRNA-treated cells. *Rad21* siRNA treatments also led to increased *Igf2* expression levels ($P < 0.05$), whereas *Smc1* siRNA had no significant effect ($P > 0.05$), probably due to an insufficient KD. Surprisingly, *H19* levels were mostly unaffected, and in *Ctcf* siRNA treatments, the levels were elevated (Fig. 5A). Next, we examined the allelic

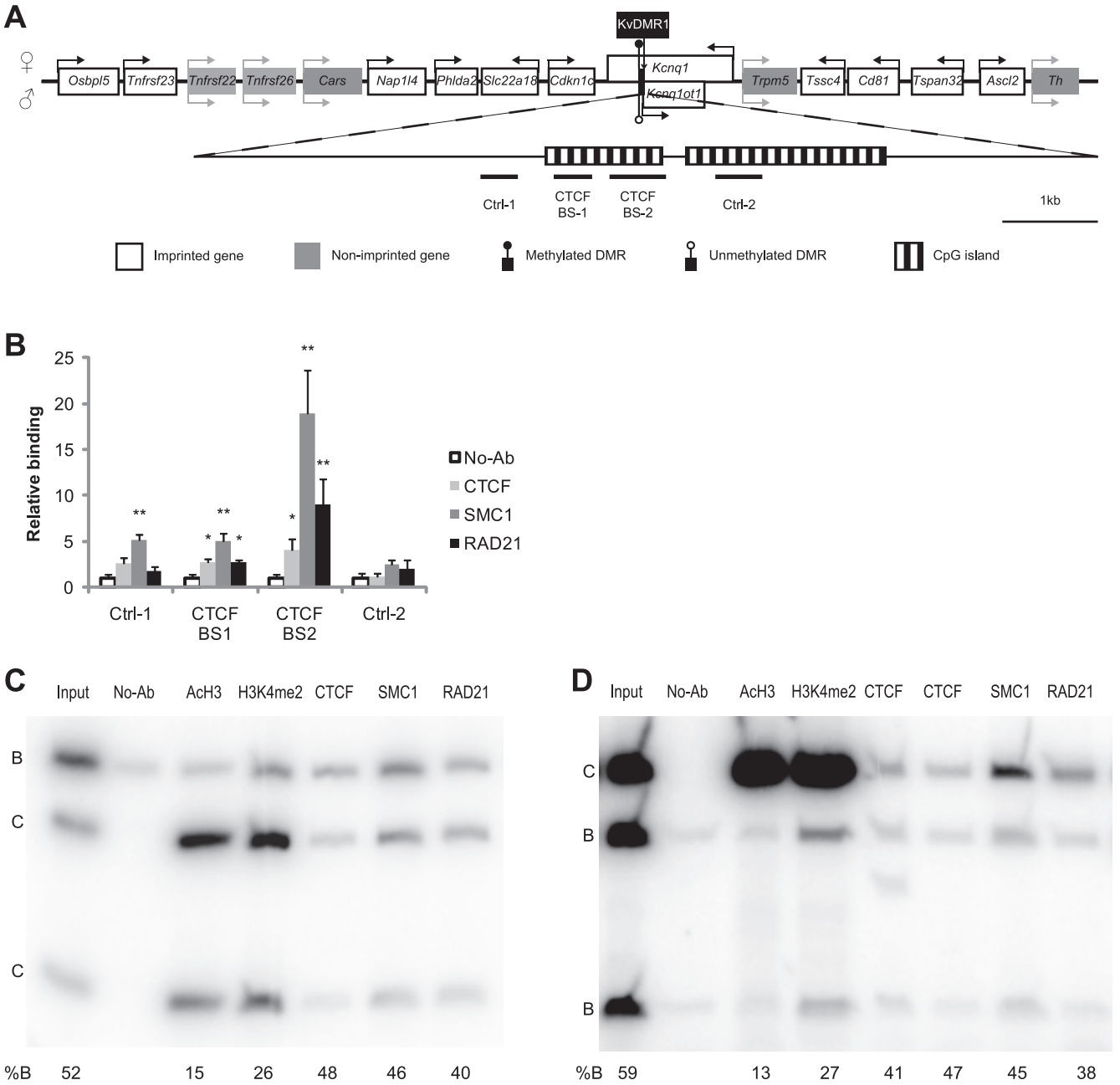

FIG. 2. CTCF and cohesins colocalize at KvDMR1 in MEFs. (A) Schematic showing the *Kcnq1*/*Kcnq1ot1* locus. The transcriptional and methylation statuses of the maternal and paternal chromosomes are represented at the top and bottom of the DNA strand, respectively. The KvDMR1 region is enlarged at the bottom. The regions analyzed in B, C, and D are indicated below the diagram. (B) ChIPs followed by real-time PCR. *, $P < 0.05$; **, $P < 0.01$. *P* values show differences between no-antibody (No-Ab) controls and antibodies against proteins of interest. The data are normalized to the no-antibody controls of each PCR. Error bars indicate standard errors of data from at least three biological replicates. (C and D) Allele-specific analysis of ChIPed DNA by PCR showing binding of CTCF and cohesins in KvDMR1. (C) CTCF BS-1; (D) CTCF BS-2. AcH3 and H3K4me2 are included as controls. B, maternal allele; C, paternal allele. The percentage of protein binding on the B allele over total binding (B plus C) is indicated at the bottom. At least three experiments were performed, and similar results were obtained.

expression of *Igf2* and *H19*. Unexpectedly, most cells maintained imprinted *Igf2* and *H19* expressions (Fig. 5B and data not shown). When biallelic *Igf2* expression was observed, the maternal expression level was very low (Fig. 5B, arrowhead). Because *Igf2* levels were increased ~3-fold compared to those of controls, we concluded that the enrichment was not from the normally silent maternal allele but rather from the normally active paternal allele. One possible explanation is that the residual amount of CTCF is sufficient to maintain imprinting.

To test whether the above-described phenotype depends on the CTCF-binding sites in the *H19* ICR, we conducted

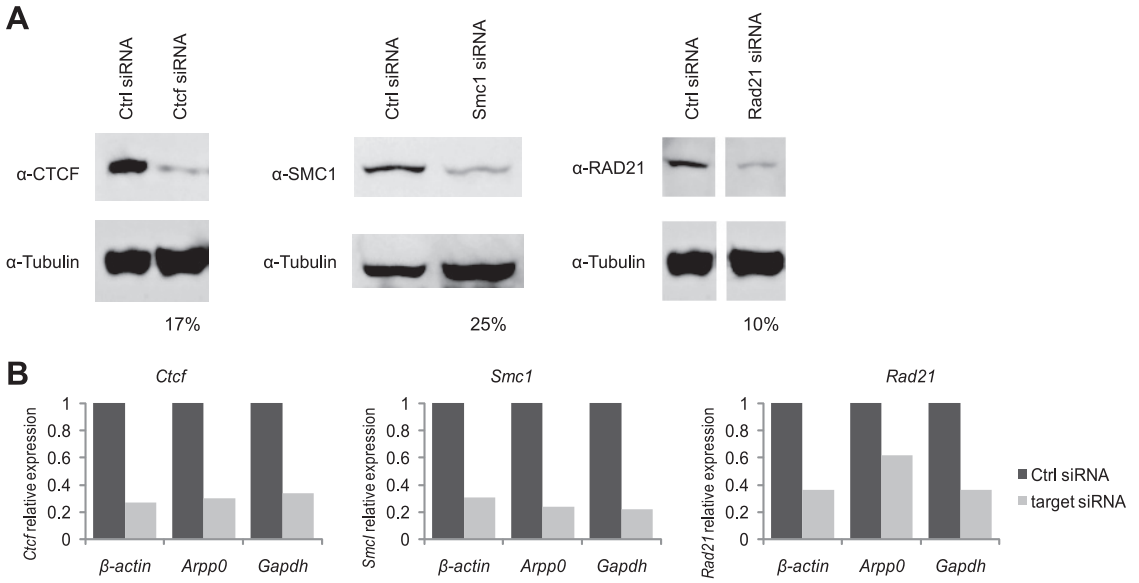

FIG. 3. Successful depletion of CTCF, SMC1, and RAD21 from MEFs. (A) Western blots showing 75% to 90% depletion of CTCF and cohesin complex subunits by siRNA treatments. MEFs were treated twice (48 h apart), and cell lysates were collected at 96 h. α-Tubulin was used as a control. (B) *Ctcf*, *Smc1*, and *Rad21* mRNA levels were normalized to three housekeeping genes, the β-actin, *Arpp0*, and GAPDH genes.

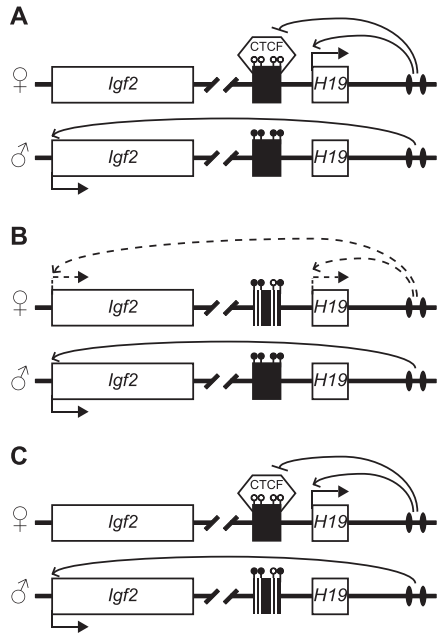

FIG. 4. MEFs used for functional analysis of CTCF and cohesins. Schematics show the *H19*/*Igf2* locus (not to scale). The black rectangle represents the *H19* ICR. Open lollipops represent unmethylated DNA; closed lollipops represent methylated DNA. (A) On the wild-type locus, the ICR exhibits paternal-specific methylation and contains binding sites for CTCF. On the maternal allele, CTCF binds to the ICR and blocks the *Igf2* promoter from accessing the 3′ shared enhancers. On the paternal allele, the ICR is methylated, and *H19* transcription is repressed. Because CTCF binding is methylation sensitive, the ICR cannot act as an insulator on the paternal allele, allowing *Igf2* expression. (B and C) In the $H19^{\Delta R}$ MEFs, four CTCF-binding sites in the ICR are deleted (white bars). (B) Upon maternal transmission of the mutant allele, the insulator activity is lost because CTCF cannot bind to the ICR, *Igf2* exhibits biallelic expression, and the *H19* expression level is reduced (12). (C) Upon paternal transmission of the mutant allele, *H19* remains monoallelically expressed, and the *Igf2* expression level is similar to that of the wild-type (12).

siRNA treatments of MEFs that harbor the $H19^{\Delta R}$ mutant allele (12). When the mutant allele was transmitted maternally, the insulator function at the maternal *H19* ICR was disrupted due to the deletion of the four CTCF-binding sites at the endogenous locus (Fig. 4B), leading to biallelic *Igf2* expression (12) (Fig. 5D). In contrast, when the mutant allele was transmitted paternally, the normal imprinted expression of *H19* and *Igf2* was maintained (12) (Fig. 4C and 5F). If the phenotype in the wild-type cells (Fig. 5A and B) depended on the maternal CTCF-binding sites in the *H19* ICR, we would expect to see no changes in *H19* and *Igf2* expression in the $H19^{\Delta R/+}$ cells. Contrary to our expectation, the depletion of CTCF resulted in increased *Igf2* expression levels in KD $H19^{\Delta R/+}$ MEFs (Fig. 5C). When both SMC1 and RAD21 were depleted in these cells, the *Igf2* expression level was increased (Fig. 5C). Furthermore, an allele-specific analysis showed that *Igf2* expression remained biallelic (Fig. 5D) (i.e., there was no difference compared to control siRNA-treated cells), indicating that the activation was on both alleles in the $H19^{\Delta R/+}$ MEFs. In $H19^{+/\Delta R}$ MEFs, the depletion of CTCF also caused elevated *Igf2* expression levels but not a loss of imprinting (Fig. 5E and F). We conclude that CTCF has repressive functions on *Igf2* expression independent of the CTCF-binding sites in the *H19* ICR. The role of cohesins in the repression of *Igf2* was not as pronounced and likely indirect.

We also examined five imprinted genes in the *Dlk1-Dio3* and the *Kcnq1*/*Kcnq1ot1* loci in the CTCF KD and cohesin KD MEFs. No loss of imprinting was observed for *Dlk1*, *Gtl2*, *Kcnq1*, *Kcnq1ot1*, and *Cdkn1c* (data not shown). Although the expression levels of *Dlk1* and *Gtl2* were not affected in most siRNA treatments, when a difference was observed, it was always an increase in expression levels (Fig. 6A). No significant difference in the *Kcnq1ot1* expression level was observed (Fig. 6B).

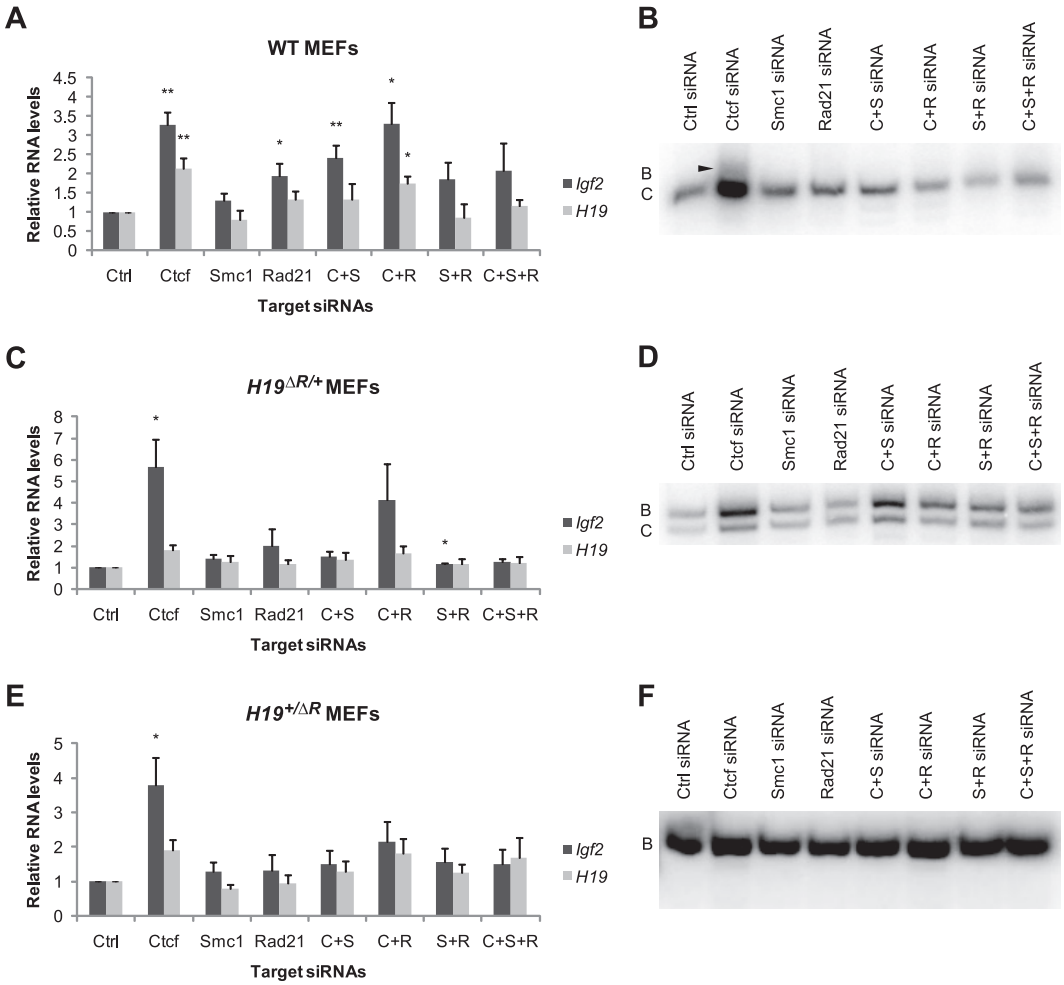

FIG. 5. Depletion of CTCF and cohesins associated with elevated *Igf2* expression levels. (A) Relative RNA levels of *H19* and *Igf2* in siRNA-treated wild-type (WT) MEFs. *, $P < 0.05$; **, $P < 0.01$. *P* values show differences between CTCF or cohesin siRNA treatments and the control siRNA treatment. *H19* and *Igf2* RNA levels are normalized to *Arpp0*. The relative value of the control siRNA treatment is set to 1. Error bars indicate standard errors. C, Ctcf siRNA; S, Smc1 siRNA; R, Rad21 siRNA. (B) Allele-specific analysis of *Igf2* RNA in wild-type MEFs. Samples were collected at 144 h after three sequential treatments with siRNAs. Only the second lane had a low level of maternal *Igf2* expression detected (arrowhead). B, maternal allele; C, paternal allele. (C) *H19* and *Igf2* relative RNA levels in siRNA-treated $H19^{\Delta R/+}$ MEFs. *, $P < 0.05$. The *P* value shows the difference between CTCF siRNA treatments and the control siRNA treatment. *H19* and *Igf2* RNA levels are normalized to *Arpp0*. The relative value of the control siRNA treatment was set to 1. Error bars indicate standard errors. (D) Allele-specific analysis of *Igf2* RNA in $H19^{\Delta R/+}$ MEF cells. Samples were collected at 96 h after two sequential treatments of siRNAs. All samples have similar amounts of B (maternal) and C (paternal) alleles. (E) *H19* and *Igf2* relative RNA levels in siRNA-treated $H19^{+/\Delta R}$ MEFs. *, $P < 0.05$. The *P* value shows the difference between CTCF or cohesin siRNA treatments and the control siRNA treatment. *H19* and *Igf2* RNA levels are normalized to *Arpp0*. The relative value of the control siRNA treatment was set to 1. Error bars indicate standard errors. (F) Allele-specific analysis of *Igf2* RNA in $H19^{+/\Delta R}$ MEFs. Samples were collected at 120 h after two sequential treatments of siRNAs. All samples have monoallelic expression of the B (paternal) allele.

DISCUSSION

The first evidence for noncanonical functions of cohesins came from human diseases associated with mutations in cohesins and cohesin-related genes. Mutations in the *NIPBL* gene (the human ortholog of *Scc2*, which loads cohesins onto chromatin [7]) and, subsequently, in the *SMC1A* and *SMC3* genes of Cornelia de Lange syndrome (CdLS) patients were described previously (8, 30, 62). Surprisingly, some CdLS individuals do not have severe defects in sister chromatid cohesion (28), suggesting that cohesins are involved in gene regulation and development independent of their mitotic role. Following this discovery, a number of studies revealed that cohesins were required in neuronal morphogenesis and embryonic development in model organisms (for a review, see reference 1). Although cohesins can function as transcriptional activators at some genes, they may repress the expression of other genes (1). The possible mechanism(s) by which cohesins carry out distinct functions at different genes remained unknown until the genome-wide colocalization of cohesins and CTCF was described (43, 48, 67). Consistent with the idea that CTCF and cohesins function cooperatively in transcriptional regulation, we found a colocalization of CTCF and cohesins at three imprinted loci and observed similar changes in imprinted gene RNA levels between CTCF KD and cohesin KD cells

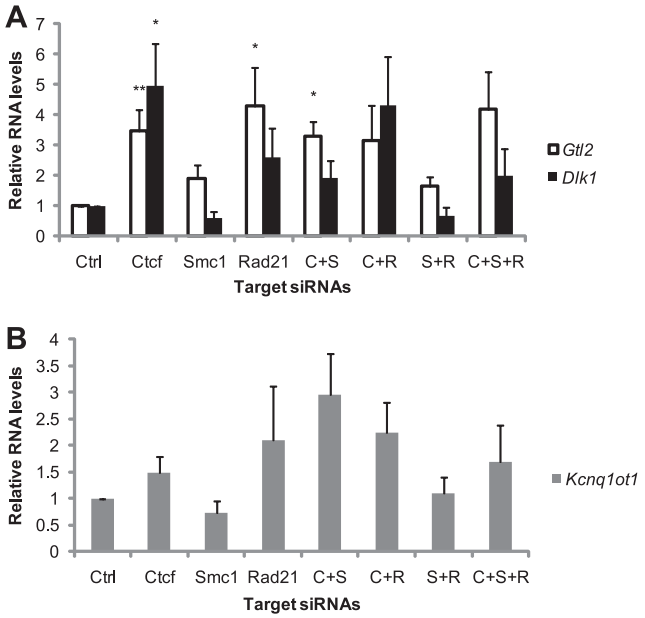

FIG. 6. Depletion of CTCF and cohesins leads to changes in *Gtl2* and *Dlk1* expression but not in *Kcnq1ot1* RNA levels. (A) Relative RNA levels of *Gtl2* and *Dlk1* in siRNA-treated MEF cells. *, $P < 0.05$; **, $P < 0.01$. *P* values reflect the differences between CTCF or cohesin siRNA treatments and the control siRNA treatment. (B) Relative RNA levels of *Kcnq1ot* in siRNA-treated MEF cells. No significant change was seen between CTCF or cohesin siRNA treatments and the control siRNA treatment. For both panels, the levels of imprinted gene RNA were normalized to *Arpp0*. The relative value of the control siRNA treatment was set to 1. Error bars indicate standard errors.

(Fig. 5 and 6). However, the CTCF KD had a much stronger effect than did the cohesin KD (Fig. 5 and 6). Therefore, we cannot rule out the possibility that cohesins do not have direct roles at imprinted loci and function independently of CTCF. In addition to CTCF, other partners of cohesins in gene regulation have been described, including the Polycomb protein complex PRC2 (49), the Mediator complex (26), and estrogen receptor (ER) alpha (50). The Mediator- and ER-associated sites are largely depleted of CTCF-associated cohesin-binding sites (26, 50), suggesting that cohesins function through distinct cofactors. Nevertheless, the colocalization of the binding of CTCF and cohesins at imprinted loci and the similar effects seen upon KD suggest that CTCF and cohesins cooperate in regulating the expression of imprinted genes.

CTCF's role at the *H19* ICR as an insulator protein regulating genomic imprinting is well established (for a review, see reference 2). When CTCF-binding sites in the *H19* ICR are deleted from the maternal chromosome, the insulator activity is lost, resulting in the biallelic expression of *Igf2* and reduced *H19* expression levels (12). However, we did not observe a loss of insulation at the *H19* ICR in MEFs when CTCF was depleted by RNAi (Fig. 4C and E), nor did we see a reduction in *H19* RNA levels. This finding could be attributed to our KD experiments not reducing CTCF below a threshold level required to maintain insulation at the *H19* ICR in MEFs. Alternatively, CTCF may be required only for the establishment, rather than the maintenance, of *Igf2* imprinting. Our previous work, however, argues against this idea. The conditional deletion of the entire *H19* ICR from the mouse neonatal liver led to a loss of imprinting, suggesting that the ICR is required to maintain *Igf2* repression on the maternal allele (60). Nevertheless, the presence of CTCF prior to the RNAi treatment could be sufficient for establishing a chromatin state that is able to maintain imprinted gene expression. The fact that we observed increased expression levels of *Igf2* and *H19* RNAs upon the depletion of CTCF (Fig. 5A) suggests that CTCF has dual functions in the regulation of the *H19*/*Igf2* locus, namely, insulation and transcriptional repression.

Similar experiments involving the depletion of CTCF and cohesin complex subunits by siRNA or short hairpin RNA (shRNA) treatments have been reported in the literature. Wendt et al. showed a reduction of *H19* RNA levels and increased *Igf2* RNA levels upon the depletion of both CTCF and RAD21 in HeLa cells (67). However, neither a statistical analysis of the mRNA changes nor an allele-specific expression analysis was performed in that study. Furthermore, Nativio et al. reported no changes in *H19* imprinted expression or total *H19* RNA in human HB2 cells. The authors described elevated and biallelic expression of *Igf2* after RAD21 KD, but the level was so low prior to KD that it was impossible to determine whether basal transcription was monoallelic or biallelic (42). The disparity between data from these studies and data from our study could originate from differences in cell types and species (mouse versus human). A recent study using MEFs by Yao et al. showed reduced *H19* and increased *Igf2* expression levels upon CTCF depletion by shRNA (69). However, the reduction of the *H19* expression level was not statistically significant, and those authors did not show the allelic expression profile of *Igf2*, leaving the underlying mechanism for the phenotypes unclear. Thus, the role of cohesins in insulator function at the *H19* ICR remains uncertain.

Despite the disparate observations in our study and the ones described above (42, 67, 69), one phenotype is strikingly similar, namely, elevated *Igf2* RNA levels after the depletion of CTCF and cohesins, which is independent of the CTCF-binding sites in the *H19* ICR (Fig. 5). ChIP assays with various human and mouse tissues revealed multiple CTCF-binding sites at the *Igf2* locus (6, 11, 31, 33, 71); CTCF appears preferentially bound to the maternal allele of *Igf2* DMR1 and the P2 and P3 promoters (31, 33). Although those observations suggest that CTCF is involved in the maternal-specific repression of *Igf2*, our data argue against this idea. Additional CTCF-binding sites at the mouse *Igf2* locus have been reported. One report stated that CTCF binds to *Igf2* DMR0, which is largely placenta specific (41), on both alleles (33), whereas we detected no binding in MEFs (data not shown). In concordance with the latter observation, we saw no consistent enhanced expression from the *Igf2* P0 promoter in KD MEFs (data not shown). Other sites, which are located 5.2 kb and 1.7kb upstream of the *Igf2* DMR0, have not been tested allelically (6, 71), but SMC1 also binds to these sites in MEFs (Gene Expression Omnibus [GEO] accession number GSM560355) (26). Finally, CTCF and SMC3 bind upstream of human *Igf2* DMR0 on both parental alleles (42). We hypothesized that the CTCF-binding sites in the *H19* ICR have a higher affinity for CTCF and/or cohesins than the binding sites at *Igf2* and that the depletion of CTCF and RAD21 causes a loss of binding at *Igf2* but not the *H19* ICR. Therefore, only the repressive func-

tion but not the insulator function is disturbed upon siRNA treatment. To test this idea, we performed ChIP experiments on MEFs treated with control and *Ctcf* siRNAs. In *Ctcf* siRNA-treated MEFs, CTCF, SMC1, and RAD21 remained bound at the *H19* ICR and at both sites upstream of *Igf2* DMR0 (data not shown). Therefore, it is unlikely that CTCF functions through these binding sites to repress *Igf2* expression.

Although the role of CTCF at the *H19*/*Igf2* locus is well established, its functions at the *Gtl2* DMR and KvDMR1 remain to be elucidated. The colocalization of CTCF and cohesins at these DMRs suggests that the proteins function together. Although we did not observe a loss of imprinting in any genes tested following the depletion of CTCF and cohesin in MEFs, mRNA levels of imprinted genes were either increased or unaltered (Fig. 4C and E and 5), suggesting a role in the repression of some genes at these loci. An elucidation of the function at these loci is complicated by the fact that CTCF and cohesins bind to thousands of genomic sites. The mechanism(s) by which CTCF and cohesins impact gene expression at imprinted loci other than the *H19*/*Igf2* locus is unclear. Interestingly, the depletion of both CTCF and cohesins similarly affects the genes in the *H19*/*Igf2* and *Dlk1*/*Gtl2* imprinted clusters (Fig. 5A and 6A).

The above-mentioned results suggest the following possible mechanisms. First, CTCF and cohesins function in concert to regulate a transcriptional activator or repressor. The removal of CTCF and cohesins would increase the activity of an activator (or diminish the activity of a repressor), which would lead to the overexpression of imprinted genes in the same cluster. Second, given that CTCF mediates inter- and intrachromosomal interactions (for a review, see reference 68) and is enriched at nuclear lamina-associated domains (18), CTCF and cohesins would participate in the higher chromosome organization that is required to localize gene loci to certain domains in the nucleus. The loss of CTCF and cohesins may therefore impair this chromatin organization, leading to elevated expression levels of imprinted genes. Third, CTCF and cohesins could function through the imprinted gene network (IGN). The IGN was first described in a microarray analysis that suggested a coregulation of imprinted genes (63). Interestingly, *H19*, *Igf2*, and *Dlk1* expression levels are co-upregulated or downregulated in *Zac1*-overexpressed or -depleted tissues, respectively (63). Additional evidence for the IGN came from a study showing the coordinated downregulation of 11 imprinted genes (including *H19*, *Igf2*, *Dlk1*, and *Gtl2*) independent of DNA methylation during postnatal growth deceleration in various mouse tissues (37). Furthermore, *Cdkn1c*, an imprinted gene in the *Kcnq1*/*Kcnq1ot* cluster, was also identified as a member of the IGN in those two studies (37, 63). It is possible that CTCF and cohesins play a role in the IGN because of their binding patterns in various related genes. However, the mechanism underlying IGN gene cross talk and coregulation remains to be elucidated.

The complexity of CTCF and cohesins is further highlighted due to their cell-type-specific binding patterns. ChIPs targeting CTCF and cohesins in various cell types revealed different binding profiles (14, 26, 49, 50). A previous analysis by Essien et al. suggested that CTCF-binding sites at the imprinted loci described here had a relatively low affinity for CTCF (14). These low-occupancy CTCF-binding sites tend to be cell type specific and developmentally regulated (14). Similarly, cohesins also have different binding profiles between mouse embryonic stem cells and MEFs (26) as well as among different human tissues (50) and *Drosophila* cell lines (49). Those observations suggest that CTCF and cohesins have distinct functions in different cell types at a subset of targets. To illustrate further the roles of CTCF and cohesins in genomic imprinting, more cell types need to be investigated. By comparing the binding profiles of CTCF and cohesins at imprinted loci in different cell types, and subsequently correlating these with the imprinted gene expression patterns, one would be able to determine which binding sites are controlling imprinting and which are controlling transcriptional levels.

In conclusion, our results have provided a systematic view of the colocalization of CTCF and cohesins at imprinted gene loci. Distinct binding profiles of CTCF and cohesins at different imprinted DMRs indicate locus-specific functions. Furthermore, by performing our allele-specific analysis, we have uncovered new roles for CTCF in the transcription regulation of the active allele of imprinted genes. Our findings also suggest a role for cohesins in regulating the expression of imprinted genes.

ACKNOWLEDGMENTS

We thank D. N. Filippova for the siRNA protocol. We thank the members of Bartolomei laboratory for their helpful discussion of this work and critical reading of the manuscript.

This research was supported by the National Institutes of Health (grants HD042026 to M.S.B. and R.M.S., GM51270 to M.S.B., and HD022681 to R.M.S.) and the Medical Research Council, United Kingdom (A.C.F.-S.).

REFERENCES

1. **Barbero, J. L.** 2009. Cohesins: chromatin architects in chromosome segregation, control of gene expression and much more. Cell. Mol. Life Sci. **66:**2025–2035.
2. **Bartolomei, M. S.** 2009. Genomic imprinting: employing and avoiding epigenetic processes. Genes Dev. **23:**2124–2133.
3. **Bell, A. C., and G. Felsenfeld.** 2000. Methylation of a CTCF-dependent boundary controls imprinted expression of the *Igf2* gene. Nature **405:**482–485.
4. **Butler, M. G.** 2009. Genomic imprinting disorders in humans: a mini-review. J. Assist. Reprod. Genet. **26:**477–486.
5. **Carr, M. S., A. Yevtodiyenko, C. L. Schmidt, and J. V. Schmidt.** 2007. Allele-specific histone modifications regulate expression of the *Dlk1-Gtl2* imprinted domain. Genomics **89:**280–290.
6. **Chen, X., et al.** 2008. Integration of external signaling pathways with the core transcriptional network in embryonic stem cells. Cell **133:**1106–1117.
7. **Ciosk, R., et al.** 2000. Cohesin's binding to chromosomes depends on a separate complex consisting of Scc2 and Scc4 proteins. Mol. Cell **5:**243–254.
8. **Deardorff, M., et al.** 2007. Mutations in cohesin complex members SMC3 and SMC1A cause a mild variant of Cornelia de Lange syndrome with predominant mental retardation. Am. J. Hum. Genet. **80:**485–494.
9. **Dorsett, D.** 2007. Roles of the sister chromatid cohesion apparatus in gene expression, development, and human syndromes. Chromosoma **116:**1–13.
10. **Dorsett, D., et al.** 2005. Effects of sister chromatid cohesion proteins on cut gene expression during wing development in Drosophila. Development **132:**4743–4753.
11. **Du, M., et al.** 2003. Insulator and silencer sequences in the imprinted region of human chromosome 11p15.5. Hum. Mol. Genet. **12:**1927–1939.
12. **Engel, N., J. L. Thorvaldsen, and M. S. Bartolomei.** 2006. CTCF-binding sites promote transcription initiation and prevent DNA methylation on the maternal allele at the imprinted *H19*/*Igf2* locus. Hum. Mol. Genet. **15:**2945–2954.
13. Reference deleted.
14. **Essien, K., et al.** 2009. CTCF-binding site classes exhibit distinct evolutionary, genomic, epigenomic and transcriptomic features. Genome Biol. **10:**R131.
15. **Filippova, G. N.** 2008. Genetics and epigenetics of the multifunctional protein CTCF. Curr. Top. Dev. Biol. **80:**337–360.
16. **Fitzpatrick, G. V., et al.** 2007. Allele-specific binding of CTCF to the multipartite imprinting control region KvDMR1. Mol. Cell. Biol. **27:**2636–2647.

17. **Fitzpatrick, G. V., P. D. Soloway, and M. J. Higgins.** 2002. Regional loss of imprinting and growth deficiency in mice with a targeted deletion of KvDMR1. Nat. Genet. **32:**426–431.
18. **Guelen, L., et al.** 2008. Domain organization of human chromosomes revealed by mapping of nuclear lamina interactions. Nature **453:**948–951.
19. **Haering, C. H., A. Farcas, P. Arumugam, J. Metson, and K. Nasmyth.** 2008. The cohesin ring concatenates sister DNA molecules. Nature **454:**297–301.
20. **Hagan, J. P., B. L. O'Neill, C. L. Stewart, S. V. Kozlov, and C. M. Croce.** 2009. At least ten genes define the imprinted *Dlk1-Dio3* cluster on mouse chromosome 12qF1. PLoS One **4:**e4352.
21. **Hark, A. T., et al.** 2000. CTCF mediates methylation-sensitive enhancer-blocking activity at the *H19*/*Igf2* locus. Nature **405:**486–489.
22. **Hikichi, T., T. Kohda, T. Kaneko-Ishino, and F. Ishino.** 2003. Imprinting regulation of the murine *Meg1*/*Grb10* and human *GRB10* genes; roles of brain-specific promoters and mouse-specific CTCF-binding sites. Nucleic Acids Res. **31:**1398–1406.
23. **Kagami, M., et al.** 2005. Segmental and full paternal isodisomy for chromosome 14 in three patients: narrowing the critical region and implication for the clinical features. Am. J. Med. Genet. **138A:**127–132.
24. **Kagami, M., et al.** 2010. The IG-DMR and the MEG3-DMR at human chromosome 14q32.2: hierarchical interaction and distinct functional properties as imprinting control centers. PLoS Genet. **6:**e1000992.
25. **Kagami, M., et al.** 2008. Deletions and epimutations affecting the human 14q32.2 imprinted region in individuals with paternal and maternal upd(14)-like phenotypes. Nat. Genet. **40:**237–242.
26. **Kagey, M. H., et al.** 2010. Mediator and cohesin connect gene expression and chromatin architecture. Nature **467:**430–435.
27. **Kanduri, C., et al.** 2000. Functional association of CTCF with the insulator upstream of the *H19* gene is parent of origin-specific and methylation-sensitive. Curr. Biol. **10:**853–856.
28. **Kaur, M., et al.** 2005. Precocious sister chromatid separation (PSCS) in Cornelia de Lange syndrome. Am. J. Med. Genet. **138A:**27–31.
29. **Kernohan, K. D., et al.** 2010. ATRX partners with cohesin and MeCP2 and contributes to developmental silencing of imprinted genes in the brain. Dev. Cell **18:**191–202.
30. **Krantz, I. D., et al.** 2004. Cornelia de Lange syndrome is caused by mutations in NIPBL, the human homolog of Drosophila melanogaster Nipped-B. Nat. Genet. **36:**631–635.
31. **Kurukuti, S., et al.** 2006. CTCF binding at the *H19* imprinting control region mediates maternally inherited higher-order chromatin conformation to restrict enhancer access to *Igf2*. Proc. Natl. Acad. Sci. U. S. A. **103:**10684–10689.
32. **Lewis, A., et al.** 2004. Imprinting on distal chromosome 7 in the placenta involves repressive histone methylation independent of DNA methylation. Nat. Genet. **36:**1291–1295.
33. **Li, T., et al.** 2008. CTCF regulates allelic expression of *Igf2* by orchestrating a promoter-polycomb repressive complex 2 intrachromosomal loop. Mol. Cell. Biol. **28:**6473–6482.
34. **Lin, S., et al.** 2007. Differential regulation of imprinting in the murine embryo and placenta by the *Dlk1-Dio3* imprinting control region. Development **134:**417–426.
35. **Lin, S., et al.** 2003. Asymmetric regulation of imprinting on the maternal and paternal chromosomes at the *Dlk1-Gtl2* imprinted cluster on mouse chromosome 12. Nat. Genet. **35:**97–102.
36. **Lobanenkov, V. V., et al.** 1990. A novel sequence-specific DNA binding protein which interacts with three regularly spaced direct repeats of the CCCTC-motif in the 5′-flanking sequence of the chicken *c-myc* gene. Oncogene **5:**1743–1753.
37. **Lui, J. C., G. P. Finkielstain, K. M. Barnes, and J. Baron.** 2008. An imprinted gene network that controls mammalian somatic growth is down-regulated during postnatal growth deceleration in multiple organs. Am. J. Physiol. Regul. Integr. Comp. Physiol. **295:**R189–R196.
38. **Mancini-DiNardo, D., S. J. S. Steele, R. S. Ingram, and S. M. Tilghman.** 2003. A differentially methylated region within the gene *Kcnq1* functions as an imprinted promoter and silencer. Hum. Mol. Genet. **12:**283–294.
39. **Mancini-Dinardo, D., S. J. S. Steele, J. M. Levorse, R. S. Ingram, and S. M. Tilghman.** 2006. Elongation of the *Kcnq1ot1* transcript is required for genomic imprinting of neighboring genes. Genes Dev. **20:**1268–1282.
40. **Mann, M. R. W., et al.** 2003. Disruption of imprinted gene methylation and expression in cloned preimplantation stage mouse embryos. Biol. Reprod. **69:**902–914.
41. **Moore, T., et al.** 1997. Multiple imprinted sense and antisense transcripts, differential methylation and tandem repeats in a putative imprinting control region upstream of mouse Igf2. Proc. Natl. Acad. Sci. U. S. A. **94:**12509–12514.
42. **Nativio, R., et al.** 2009. Cohesin is required for higher-order chromatin conformation at the imprinted *IGF2-H19* locus. PLoS Genet. **5:**e1000739.
43. **Parelho, V., et al.** 2008. Cohesins functionally associate with CTCF on mammalian chromosome arms. Cell **132:**422–433.
44. **Pateras, I. S., K. Apostolopoulou, K. Niforou, A. Kotsinas, and V. G. Gorgoulis.** 2009. p57KIP2: "Kip"ing the cell under control. Mol. Cancer Res. **7:**1902–1919.
45. **Paulsen, M., et al.** 2001. Comparative sequence analysis of the imprinted *Dlk1-Gtl2* locus in three mammalian species reveals highly conserved genomic elements and refines comparison with the *Igf2-H19* region. Genome Res. **11:**2085–2094.
46. **Reese, K. J., S. Lin, R. I. Verona, R. M. Schultz, and M. S. Bartolomei.** 2007. Maintenance of paternal methylation and repression of the imprinted *H19* gene requires MBD3. PLoS Genet. **3:**e137.
47. **Rollins, R. A., M. Korom, N. Aulner, A. Martens, and D. Dorsett.** 2004. Drosophila nipped-B protein supports sister chromatid cohesion and opposes the stromalin/Scc3 cohesion factor to facilitate long-range activation of the cut gene. Mol. Cell. Biol. **24:**3100–3111.
48. **Rubio, E. D., et al.** 2008. CTCF physically links cohesin to chromatin. Proc. Natl. Acad. Sci. U. S. A. **105:**8309–8914.
49. **Schaaf, C. A., et al.** 2009. Regulation of the Drosophila Enhancer of split and invected-engrailed gene complexes by sister chromatid cohesion proteins. PLoS One **4:**e6202.
50. **Schmidt, D., et al.** 2010. A CTCF-independent role for cohesin in tissue-specific transcription. Genome Res. **20:**578–588.
51. **Schuster-Gossler, K., P. Bilinski, T. Sado, A. Ferguson-Smith, and A. Gossler.** 1998. The mouse *Gtl2* gene is differentially expressed during embryonic development, encodes multiple alternatively spliced transcripts, and may act as an RNA. Dev. Dyn. **212:**214–228.
52. **Shin, J., G. V. Fitzpatrick, and M. J. Higgins.** 2008. Two distinct mechanisms of silencing by the KvDMR1 imprinting control region. EMBO J. **27:**168–178.
53. **Smilinich, N. J., et al.** 1999. A maternally methylated CpG island in *KvLQT1* is associated with an antisense paternal transcript and loss of imprinting in Beckwith-Wiedemann syndrome. Proc. Natl. Acad. Sci. U. S. A. **96:**8064–8069.
54. **Stedman, W., et al.** 2008. Cohesins localize with CTCF at the KSHV latency control region and at cellular *c-myc* and *H19*/*Igf2* insulators. EMBO J. **27:**654–666.
55. **Szabó, P. E., S. E. Tang, A. Rentsendorj, G. P. Pfeifer, and J. R. Mann.** 2000. Maternal-specific footprints at putative CTCF sites in the *H19* imprinting control region give evidence for insulator function. Curr. Biol. **10:**607–610.
56. **Takada, S., et al.** 2000. *Delta-like* and *Gtl2* are reciprocally expressed, differentially methylated linked imprinted genes on mouse chromosome 12. Curr. Biol. **10:**1135–1138.
57. **Thakur, N., M. Kanduri, C. Holmgren, R. Mukhopadhyay, and C. Kanduri.** 2003. Bidirectional silencing and DNA methylation-sensitive methylation-spreading properties of the *Kcnq1* imprinting control region map to the same regions. J. Biol. Chem. **278:**9514–9519.
58. **Thakur, N., et al.** 2004. An antisense RNA regulates the bidirectional silencing property of the *Kcnq1* imprinting control region. Mol. Cell. Biol. **24:**7855–7862.
59. **Thorvaldsen, J. L., K. L. Duran, and M. S. Bartolomei.** 1998. Deletion of the *H19* differentially methylated domain results in loss of imprinted expression of *H19* and *Igf2*. Genes Dev. **12:**3693–3702.
60. **Thorvaldsen, J. L., A. M. Fedoriw, S. Nguyen, and M. S. Bartolomei.** 2006. Developmental profile of *H19* differentially methylated domain (DMD) deletion alleles reveals multiple roles of the DMD in regulating allelic expression and DNA methylation at the imprinted *H19*/*Igf2* locus. Mol. Cell. Biol. **26:**1245–1258.
61. **Thorvaldsen, J. L., M. R. W. Mann, O. Nwoko, K. L. Duran, and M. S. Bartolomei.** 2002. Analysis of sequence upstream of the endogenous *H19* gene reveals elements both essential and dispensable for imprinting. Mol. Cell. Biol. **22:**2450–2462.
62. **Tonkin, E. T., T. Wang, S. Lisgo, M. J. Bamshad, and T. Strachan.** 2004. NIPBL, encoding a homolog of fungal Scc2-type sister chromatid cohesion proteins and fly Nipped-B, is mutated in Cornelia de Lange syndrome. Nat. Genet. **36:**636–641.
63. **Varrault, A., et al.** 2006. *Zac1* regulates an imprinted gene network critically involved in the control of embryonic growth. Dev. Cell **11:**711–722.
64. **Verona, R. I., J. L. Thorvaldsen, K. J. Reese, and M. S. Bartolomei.** 2008. The transcriptional status but not the imprinting control region determines allele-specific histone modifications at the imprinted *H19* locus. Mol. Cell. Biol. **28:**71–82.
65. **Wan, L., et al.** 2008. Maternal depletion of CTCF reveals multiple functions during oocyte and preimplantation embryo development. Development **135:**2729–2738.
66. **Weaver, J. R., et al.** 2010. Domain-specific response of imprinted genes to reduced DNMT1. Mol. Cell. Biol. **30:**3916–3928.
67. **Wendt, K. S., et al.** 2008. Cohesin mediates transcriptional insulation by CCCTC-binding factor. Nature **451:**796–801.
68. **Williams, A., and R. A. Flavell.** 2008. The role of CTCF in regulating nuclear organization. J. Exp. Med. **205:**747–750.
69. **Yao, H., et al.** 2010. Mediation of CTCF transcriptional insulation by DEAD-box RNA-binding protein p68 and steroid receptor RNA activator SRA. Genes Dev. **24:**2543–2555.
70. **Yoon, B., et al.** 2005. *Rasgrf1* imprinting is regulated by a CTCF-dependent methylation-sensitive enhancer blocker. Mol. Cell. Biol. **25:**11184–11190.
71. **Yoon, Y. S., et al.** 2007. Analysis of the *H19ICR* insulator. Mol. Cell. Biol. **27:**3499–3510.